J Antimicrob Chemother 2011; **66**: 1696–1711
doi:10.1093/jac/dkr195 Advance Access publication 28 May 2011

Journal of Antimicrobial Chemotherapy

Daptomycin resistance mechanisms in clinically derived *Staphylococcus aureus* strains assessed by a combined transcriptomics and proteomics approach

Adrien Fischer[1]*, Soo-Jin Yang[2], Arnold S. Bayer[2–4], Ali R. Vaezzadeh[5], Sébastien Herzig[1], Ludwig Stenz[1], Myriam Girard[1], George Sakoulas[6], Alexander Scherl[7], Michael R. Yeaman[2–4], Richard A. Proctor[8], Jacques Schrenzel[1] and Patrice François[1]

[1]Genomic Research Laboratory, University Hospitals of Geneva and University of Geneva, Geneva, Switzerland; [2]LA Biomedical Research Institute, Torrance, CA, USA; [3]Division of Infectious Diseases, Harbor-UCLA Medical Center, Torrance, CA, USA; [4]Geffen School of Medicine at UCLA, Los Angeles, CA, USA; [5]Harvard Medical School, Boston, MA, USA; [6]Sharp Medical Center, San Diego, CA, USA; [7]BPRG, University Hospitals of Geneva, Geneva, Switzerland; [8]University of Wisconsin School of Medicine, Madison, WI, USA

*Corresponding author. Tel: +41-22-372-93-22; Fax: +41-22-372-98-30; E-mail: adrien.fischer@genomic.ch

Received 3 February 2011; returned 24 March 2011; revised 18 April 2011; accepted 19 April 2011

Objectives: The development of daptomycin resistance in *Staphylococcus aureus* is associated with clinical treatment failures. The mechanism(s) of such resistance have not been clearly defined.

Methods: We studied an isogenic daptomycin-susceptible (DAP^S) and daptomycin-resistant (DAP^R) *S. aureus* strain pair (616; 701) from a patient with relapsing endocarditis during daptomycin treatment, using comparative transcriptomic and proteomic techniques.

Results: Minor differences in the genome content were found between strains by DNA hybridization. Transcriptomic analyses identified a number of genes differentially expressed in important functional categories: cell division; metabolism of bacterial envelopes; and global regulation. Of note, the DAP^R isolate exhibited reduced expression of the major cell wall autolysis gene coincident with the up-regulation of genes involved in cell wall teichoic acid production. Using quantitative (q)RT–PCR on the gene cadre putatively involved in cationic peptide resistance, we formulated a putative regulatory network compatible with microarray data sets, mainly implicating bacterial envelopes. Of interest, qRT–PCR of this same gene cadre from two distinct isogenic DAP^S/DAP^R clinical strain pairs revealed evidence of other strain–dependent networks operative in the DAP^R phenotype. Comparative proteomics of 616 versus 701 revealed a differential abundance of proteins in various functional categories, including cell wall-associated targets and biofilm formation proteins. Phenotypically, strains 616 and 701 showed major differences in their ability to develop bacterial biofilms in the presence of the antibacterial lipid, oleic acid.

Conclusions: Compatible with previous *in vitro* observations, *in vivo*-acquired DAP^R in *S. aureus* is a complex, multistep phenomenon involving: (i) strain-dependent phenotypes; (ii) transcriptome adaptation; and (iii) modification of the lipid and protein contents of cellular envelopes.

Keywords: cell wall metabolism, antibiotic resistance, biofilms, δ-haemolysis, oleic acid, microarrays, virulence, quantitative proteomics

Introduction

Daptomycin (formerly LY146032) is a cyclic lipopeptide antimicrobial that was recently approved in the USA for the treatment of a wide variety of *Staphylococcus aureus* infections [both methicillin-susceptible *S. aureus* (MSSA) and methicillin-resistant *S. aureus* (MRSA)], including skin and soft tissue infections, uncomplicated bacteraemia and right-sided endocarditis.[1] *In vitro*, this agent is rapidly bactericidal against *S. aureus* in a concentration-dependent manner.[2,3] However, clinical treatment failures due to the emergence of daptomycin-resistant (DAP^R) strains during therapy have now been described, especially in subacute and chronic infections such as osteomyelitis and endocarditis, and with prolonged daptomycin exposure.[2,4]

Daptomycin absolutely requires Ca^{2+} for activity:[5,6] while the native molecule is anionic, daptomycin is less active microbiologically (~10 times) until it is heavily calcium decorated, making this agent a *de facto* cationic antimicrobial peptide functionally.[7]

To date, no specific genetic determinant(s) of DAP^R in *S. aureus* have been universally defined in such strains, despite several well-known phenotypic correlates of DAP^R [e.g. thickened cell walls, enhanced surface charge, alterations in cell membrane (CM) fluidity, cross-resistance to host defence cationic peptides, altered CM phospholipid synthesis and/or translocations].[8] Also, previous investigations by our group and others suggested that alterations of CM fluidity may increase *S. aureus* resistance to antibacterial lipids such as oleic acid,[9] i.e. natural compounds having structural characteristics similar to the lipid moiety of daptomycin.[10] Of note, CM modification in *S. aureus* appears to affect the abilities of such strains to develop and maintain bacterial biofilms.[11,12] Importantly, resistance to glycopeptide antibiotics such as vancomycin has been linked to a number of phenotypic perturbations, including bacterial envelope changes,[13,14] the ability to produce biofilms[15] and/or differences in the cell wall peptidoglycan composition.[16] Concomitantly, we and others have confirmed that *S. aureus* DAP^R acquired either during serial *in vitro* passage or, more relevant to this investigation, emerging during daptomycin therapy features a temporal and progressive 'accumulation' of genetic polymorphisms [single nucleotide polymorphisms (SNPs)].[17] The acquisition of such SNPs has been most commonly observed within the *mprF* and/or *yyc* operons, with the former operon being important in surface positive charge maintenance, and the latter operon being a vital regulatory locus involved in CM lipid biosynthesis, cell wall homeostasis and biofilm formation.[18,19] Interestingly, these SNPs have frequently been associated with genetic 'gains in function'.[20,21]

Although such studies have been pivotal in disclosing potential phenotypic and genotypic correlates of DAP^R, the precise interaction(s) among DAP^R, CM lipid resistance, surface charge and biofilm dynamics, as well as putative DAP^R genetic 'pathways', remain to be elucidated. The overarching goal of the current study was to gain new insights into putative genetic determinants and pathways involved in the emergence of DAP^R in *S. aureus in vivo*. Thus, we undertook a combined transcriptomic–proteomic–phenotypic correlate approach to attempt further clarification of these issues.[17]

Materials and methods

Reagents and chemicals

All chemicals purchased were of the highest purity grade, unless otherwise stated. LiChrosolv water (Merck, Darmstadt, Germany) was used for the preparation of all buffers and solvents. Acetonitrile was purchased from Biosolve (Westford, MA, USA). Trifluoroacetic acid (TFA), α-cyano-4-hydroxycinnamic acid, 1,4-dithioerythritol, ammonium bicarbonate, iodoacetamide, glycine, porcine trypsin, Tris, BSA, rabbit phosphorylase b, chicken ovalbumin and bovine β-casein were from Sigma–Aldrich (St Louis, MO, USA). Immobilized pH gradient (IPG) strips and ampholines were purchased from GE Healthcare (Piscataway, NJ, USA). SDS–PAGE pre-cast gels and molecular mass markers were purchased from Bio-Rad (Hercules, CA, USA).

Bacterial strains and cultures

The two primary strains (methicillin susceptible) used in this study have been described in detail previously.[22] Strain 616 is the parental (pre-therapy) daptomycin-susceptible (DAP^S) bloodstream isolate initially obtained from a patient with endocarditis [daptomycin MIC (Etest) = 0.5 mg/L]; strain 701 is a DAP^R organism recovered during daptomycin treatment (daptomycin MIC = 2 mg/L) [although the currently accepted terminology should be 'daptomycin non-susceptibility', 'daptomycin resistance' (DAP^R) is used in this manuscript for ease of presentation]. These strains were isogenic by pulsogram as previously detailed, and were each *agr* type 2.[22] Lastly, strain 701 (but not 616) contained an SNP within the *mprF* open reading frame (ORF) (S295L), which resulted in a phenotypic 'gain in function' of the *mprF* gene as previously described, localized to the putative 'translocase' domain for flipping lysylphosphotidylglycerol from the inner CM to the outer CM.[23,24] Moreover, transmission electron microscopy (TEM) revealed this DAP^R isolate to have significantly thicker cell walls than the DAP^S parental strain.[25]

For selected and strain-dependent comparisons [multiple loci variable number tandem repeat analysis (MLVA) and quantitative (q)RT–PCR, see below], two additional DAP^S/DAP^R *S. aureus* strain pairs were utilized. Both strain pairs were obtained from patients with recalcitrant endocarditis; the clinical, phenotypic and selected genotypic details of these isolate pairs have been previously described.[26,27] Both DAP^S/DAP^R strain pairs were identical by PFGE pulsograms. They included MSSA strain pair BOY755 and BOY300, and MRSA strain pair 11-11 and REF2145, respectively.[24]

Biofilm assays

The potential impact of adaptations to daptomycin upon biofilm characteristics was assessed. *S. aureus* strains were grown in trypticase soy broth (TSB; Becton Dickinson, Le Pont de Claix, France) supplemented with 1% (w/v) glucose. Oleic acid (*cis*-9-octadecenoic acid; Sigma–Aldrich, Basel, Switzerland), used to mimic the lipid tail of daptomycin, was emulsified with TSB–glucose media (TSBglucOleic) by overnight agitation at 220 rpm in a Lab-Shaker at 37°C. Biofilm development was performed in TSBgluc (or TSBglucOleic emulsions) with 20 μL of overnight culture/mL of fresh medium (6 mL). Bacterial colonies were counted on Mueller–Hinton agar plates (MHA; Bio-Rad, Marnes-La-Coquette, France). Biofilm staining assays were performed as described previously.[11]

Bacterial counting methods

Direct counting was performed in Neubauer chambers, as previously described.[11] Determination of colony forming units was performed on MHA using a Countermat Flash colony counter (IUL, RB Scientific, Southampton, England).

Assessment of δ-haemolysin activity

As will be demonstrated below, we identified differences in *agr* expression (a key global regulon of *S. aureus*) between DAP^S and DAP^R strain pairs. To assess the phenotypic correlates of this genotypic difference, the functions of the *agr* operon were measured by δ-haemolysin production. The δ-haemolytic activities were determined by first streaking RN4220, a strain that only produces β–haemolysin, without the interference of α- and δ-haemolysins, on sheep blood agar plates.[28] Then, the test strains were streaked perpendicularly to the RN4220 streak. The β- and δ-haemolysins of *S. aureus* act synergistically in the lysis of sheep red blood cells. Therefore, δ-haemolysin produced by any test strain results in a zone of enhanced haemolysis in areas where this haemolysin overlaps with the β-haemolysin zone of the RN4220 strain. The degree of

synergistic haemolysis was graded from 0 to 4+ by one of the authors (S.-J. Y.), who was blinded as to the *agr* transcription data and strain identities.[29] All experiments were conducted at least twice on separate days.

Genotyping of *S. aureus* strains by MLVA assay

The DAP^S and DAP^R isolate pairs (616 and 701, BOY755 and BOY300, and MRSA11-11 and REF2145), previously characterized by PFGE, were additionally genotyped using a well-described MLVA assay.[30] This method assesses genomic elements that are different to those determined by PFGE. This technique affords higher resolution than traditional PFGE, as it is able to further discriminate into subclusters some isolates that appear clonal by multilocus sequence typing (MLST).[31] For clonal cluster (CC) comparisons, we utilized the following strains with well-characterized 'clonal complex' profiles: N315 and Mu50 (CC=5); COL, USA300 and NCTC 8325 (CC=8); and MW2 and MSSA476 (CC=1).

Transcriptional analyses

Microarray manufacturing and design

The microarray was manufactured by the *in situ* synthesis of 10807 60-mer long oligonucleotide probes (Agilent, Palo Alto, CA, USA), selected as previously described.[32] It covers >98% of all ORFs annotated in strains N315 and Mu50,[33] MW2[34] and COL,[35] NCTC 8325 and USA300,[36] as well as MRSA252 and MSSA476 (including their respective plasmids).[37]

Preparation of labelled nucleic acids for expression microarrays

Total RNA was purified from both early and late exponential phase bacteria grown in Mueller Hinton broth (MHB) and treated with DNase. Preparations of 5 μg of total *S. aureus* RNA were labelled with Cy-3 dCTP using the SuperScript II method (Invitrogen, Basel, Switzerland) and purified, as previously described.[38]

Purified genomic DNA from the reference sequenced strains used for the design of the microarray was labelled with Cy-5 dCTP and used in microarray normalization.[39] Mixtures of Cy5-labelled DNA and Cy3-labelled cDNA were hybridized and scanned, as previously described.[38]

Microarray analysis

Hybridization fluorescence intensities were quantified using Feature Extraction software (Agilent, version 8). Local background subtracted signals were corrected for unequal dye incorporation or unequal load of the labelled product, using a rank consistency filter and a curve-fitting algorithm per the default LOWESS (locally weighted linear regression) method. Data from three independent biological experiments were analysed using GeneSpring 8.0 (Silicon Genetics, Redwood City, CA, USA), as previously described,[38] with a 5% false discovery rate (*P* value cut-off, 0.05) and an arbitrary threshold of 1.5-fold for defining significant differences in expression ratios. The complete microarray data set is posted on the Gene Expression Omnibus database, available at http://www.ncbi.nlm.nih.gov/geo/, under accession numbers GPL7137 for the platform design and GSE28632 for the original data set.

Real-time PCR (qRT–PCR) validation

Gene-specific probes were designed using Primer Express 3.0 (Applied Biosystems) and are shown in Table 1. Oligonucleotide primers and probes obtained from Sigma or Applied Biosystems (minor groove binder coupled to dark quencher) were solubilized in water, and reactions were assembled in a one-step RT–PCR enzymatic mixture (Invitrogen, Carlsbad, Germany) in a final volume of 10 μL. Reactions were performed in a StepOne Plus instrument (Applied Biosystems), as described previously.[40] Results were normalized using intensity levels recorded for the rRNA 16S gene, as described previously.[41] These studies provided relative gene expression for DAP^R strains 701, BOY300 and REF2145 as compared with their respective parental DAP^S isolates listed above. The statistical significance of strain-specific differences in the normalized cycle threshold values for each transcript was evaluated by the paired *t*-test, and data were considered significant at *P* values <0.05.

Proteomics analyses

The complete procedure is described by Vaezzadeh *et al.*[42] Adaptations in the methods or experimental design for the current study are described below.

S. aureus strain growth conditions

Bacterial strains were grown in MHB, essentially as described previously.[38] Cells were grown for 5 h and lysed with 20 mg/L lysostaphin (Ambicin; Applied Microbiology, Tarratown, NY, USA) for 15 min at 37°C, in Tris–EDTA buffer. For preparation of crude membrane extracts, 20 mL culture aliquots were washed in 1.1 M saccharose-containing buffer and then suspended in 2 mL aliquots of the same buffer containing 50 mg/L of the hydrolytic enzyme lysostaphin for 10 min at 37°C. Protoplasts were recovered after centrifugation (30 min at 8000 **g**) and membrane pellets were obtained after ultracentrifugation at 50000 **g** for 50 min.

Sample preparation

Quantitative mass spectrometry-based proteomic experiments were performed on three independent replicates. Samples were prepared using isobaric tags iTRAQ (Applied Biosystems, Framingham, MD, USA), according to the manufacturer's protocol. Digestion was performed by trypsin at a protease-to-protein ratio of 1:25 using microwave catalysis (FUNAI, Hamburg, Germany). After digestion, the reaction was immediately quenched with 1 M formic acid.[42] For Experiment 1 (PR1), strain 616 was labelled with iTRAQ 114 and 701 with iTRAQ 117. For Experiment 2 (PR2), strain tags were crossed; strain 616 was labelled with iTRAQ 117 and 701 with iTRAQ 116. Lastly, for Experiment 3 (PR3), strain 616 was labelled with iTRAQ 116 and 701 with iTRAQ 114.

IPG-isoelectric focusing (IEF)

IPG-IEF was performed under the following conditions, in sequence: (i) an initial 30 min step at 500 V; (ii) a linear gradient from 500 V to 4 kV over 90 min; (iii) a linear gradient from 4 kV to 8 kV in 30 min; and (iv) a final step-up cycle from 8 kV to 30 kV for 30 min. Samples (200 μL) were loaded by overnight in-gel rehydration. Next, IPG strips were washed three times for 10 s each in three distinct high-boiling point petroleum ether baths to remove the paraffin oil. Each strip was then manually cut and gel pieces were placed in polypropylene tubes containing 80 μL of 0.1% TFA. After three separate 30 min incubations with 0.1% TFA, all extracts were pooled. The samples were then cleaned using an Oasis HLB μ-Elution 96-Well Plate system as per the manufacturer's protocol (Waters, USA). Purified samples were then dried by evaporation, resuspended in 25 μL HPLC buffer A (0.1% formic acid in 3% acetonitrile) and stored at −20°C.

Table 1. List of primers/probes for qRT–PCR

Primer/probe name	Sequence (5′→3′)	Dye/quencher	Length (bp)	Cf (μM)	NCBI accession no.
asp23_299_F	GTTAAGCCACCTTTCATGTCTAAGATAC		28	0.2	
asp23_390_R	AAATTAACTTTCTCTGATGAAGTTGTTGA		29	0.2	NP_375295.1
asp23_333_T	CTTCACGTGCAGCGATACCAGCAATTT	FAM/TAMRA	27	0.1	
mprF_F	TCATTGCTGCATTATCAGGTTTAGTC		28	0.2	
mprF_R	TTCCTCAGGGACACCTAAAGTTTT		29	0.2	NP_374473.1
mprF_P	ATTCCTGGTGGTTTCGGCG	FAM/3BQ1	27	0.1	
hla_337_F	ATGAGTACTTTAACTTATGGATTCAACGG		28	0.2	
hla_437_R	AGTGTATGACCAATCGAAACATTTG		29	0.2	M90536.1
hla_385_T	ACAGGAAAAATTGGCGGCCTTATTGGT	FAM/MGB	27	0.1	
rot_332_F	GAGTTAATGTCACCCAAAAGTGTTTCT		28	0.2	
rot_418_R	TTGGGAGATGTTTAGCATGAAAAA		29	0.2	NP_374872.1
rot_MGB	CAAAATTCCAAATACAGTGTCGTT	FAM/MGB	27	0.1	
saeRS_F	AAGAACATGATACCATTTACGCCTTA		28	0.2	
saeRS_R	CCTTGGACTAAATGGTTTTTTGACA		29	0.2	NP_373916.1
saeRS_P	CTTTAGGTGCAGATGACT	FAM/MGB	27	0.1	
sarA_17_F	ACATGGCAATTACAAAAATCAATGAT		28	0.2	
sarA_167_R	TCTTTCTCTTTGTTTTCGCTGATG		29	0.2	NP_373827.1
sarA_45_T	CTTTGAGTTGTTATCAATGGT	FAM/MGB	27	0.1	
sarR_F	TGAGTCTAACGAAATCTCATCTAAAGAGA		28	0.2	
sarR_R	CAATAACTGTTCTTTCGTCTTGTAAACTTC		29	0.2	NP_375408.1
sarR_P	TGCTAAGTGCTCAGAGTT	FAM/MGB	27	0.1	
sarS_552-576_F	CCACCATAAATACCCTCAAACTGTT		28	0.2	
sarS_615-638_R	TCATCTTCAGTTGAGCGTTCTTTT		29	0.2	NP_373349.1
sarS_595-613_P	AAAAAGCAAGGCTATCTAA	FAM/MGB	27	0.1	
sarT_217-241_F	AGCGTAAAAGAATTATCAAAAAAGG		28	0.2	
sarT_306-280_R	TTTTACAGAAACAACAATGATTACATT		29	0.2	NP_375610.1
sarT_243-265_P	TTACTTGAATAAATGTAGAGACC	FAM/MGB	27	0.1	

mprF, *fmtC*; *sarS*, *sarH1*; Cf, final concentration; NCBI, National Center for Biotechnology Information.

Liquid chromatography–mass spectrometry (LC–MS) and peptide analysis

A 5 μL peptide solution of each fraction was loaded in a 10 cm long column with an internal diameter of 100 μm. The elution gradient from 4% to 38% of the counter solvent (0.1% formic acid in 80% acetonitrile) was developed over 40 min and samples were eluted directly on a matrix-assisted laser desorption/ionization (MALDI) target using a spotting robot. An aqueous solution of matrix [α-cyano-4-hydroxycinnamic acid; 5 mg/mL (w/v) in 50% acetonitrile/0.1% TFA/10 mM $NH_4H_2PO_4$] was applied and dried. Peptides were analysed in MS and MS/MS modes using a 4800 MALDI–time of flight (TOF)/TOF tandem mass spectrometer (Applied Biosystems) using a neodymium-doped yttrium aluminium garnet (Nd:YAG) laser at 355 nm, operating at 200 Hz. Eight hundred and 1500 consecutive laser desorptions were accumulated for MS and MS/MS spectra, respectively. Data-dependent MS/MS analysis was performed automatically on the 15 most intense ions from MS spectra, with lysozyme C as the external control.

Protein identification

Peak lists were generated from raw data using the PeaktoMascot software, as appropriate to the instrument. The combined peak lists of all fractions of the same IPG strip were merged into a single mascot generic file (mgf) format and searched against a database containing the 2581 genome-sequenced *S. aureus* strain N315 proteins (UniProt knowledgebase; release 15.12, 15 December 2009) using Phenyx (GeneBio, Geneva, Switzerland) with parent ion tolerance set to 100 ppm. A variable amino acid modification was oxidized methionine. Trypsin was selected as the enzyme, with one potential missed cleavage, and the normal cleavage mode was used. The peptide p value was 1×10^{-2} for linear ion trap-orbitrap data. False-positive ratios were estimated using a reverse decoy database.[43] All data sets where searched once in the forward and once in the reverse database. Separate searches were used to keep the database size constant. Protein and peptide scores were then optimized to maintain a false-positive ratio <1%, biasing toward a conservative slight overestimation of the false-positive ratio.[43] For all analyses, only proteins matching two different peptide sequences were prioritized for further consideration.

Data analysis using iTRAQ quantification

Reporter-ion abundances for each identified peptide were quantified directly from peak lists using the dedicated Phenyx export. Extracted ion abundance values were corrected from isotopic impurities[44,45] and relative peptide ratios calculated by the quotient of corrected reporter-ion

abundances at an m/z ratio corresponding to the respective channels. Protein ratios were then obtained by calculating the geometric mean of all peptide ratios corresponding to a given protein.

Results

DAP^R and biofilm formation

A first step in studying the potential *in vivo* characteristics of *S. aureus* DAP^R was to investigate the potential correlation between this resistance phenotype and biofilm formation. *S. aureus* strains 616 (DAP^S) and 701 (DAP^R) were exposed to 0.1% oleic acid in microtitre plates in a biofilm assessment assay.[11] We chose oleic acid because of its similar biochemical nature to the lipid tail of daptomycin, in which the first seven carbene groups (CH_2) are similar to the first eight carbene groups (CH_2) of the daptomycin lipid tail, following the methyl terminal group in each molecule.

In the presence of oleic acid in the nutrient medium during growth in planktonic suspension, parental strain 616 cells outnumbered DAP^R 701 cells (Figure 1a and b). Both isolates produced an abundant biofilm in oleic acid-free conditions on polystyrene plates (Figure 1c). The total amount of biofilm assessed after solubilization of crystal violet appears similar for the two strains (Figure 1d). However, in the presence of oleic acid, the adherent bacterial population appeared significantly larger in the DAP^R strain than in the DAP^S strain (Figure 1d). Consequently, the proportion of bacteria in suspension appears larger for strain 616 than for strain 701, indicating an abundant release of adherent bacteria (Figure 1a and b). We also observed a totally different biofilm organization between the two isolates: while strain 616 showed a homogeneous colonization of the surface, strain 701 demonstrated large macroscopic aggregates (Figure 1c).

agr function

As shown in Figure S1 (available as Supplementary data at *JAC* Online), for the 616 versus 701 comparisons, both strains elaborated δ-haemolysin, although the parental strain appeared to produce somewhat more. In comparing BOY755 versus BOY300, δ-haemolysin production was equivalent. Of interest, parental MRSA11-11 produced extensive δ-haemolysin, while DAP^R REF2145 elaborated very little δ-haemolysin.

Genotypic characterization of the isolate set

MLVA revealed that the three strain sets were strictly clonal, but differed from each other in dendrogram analysis (data not

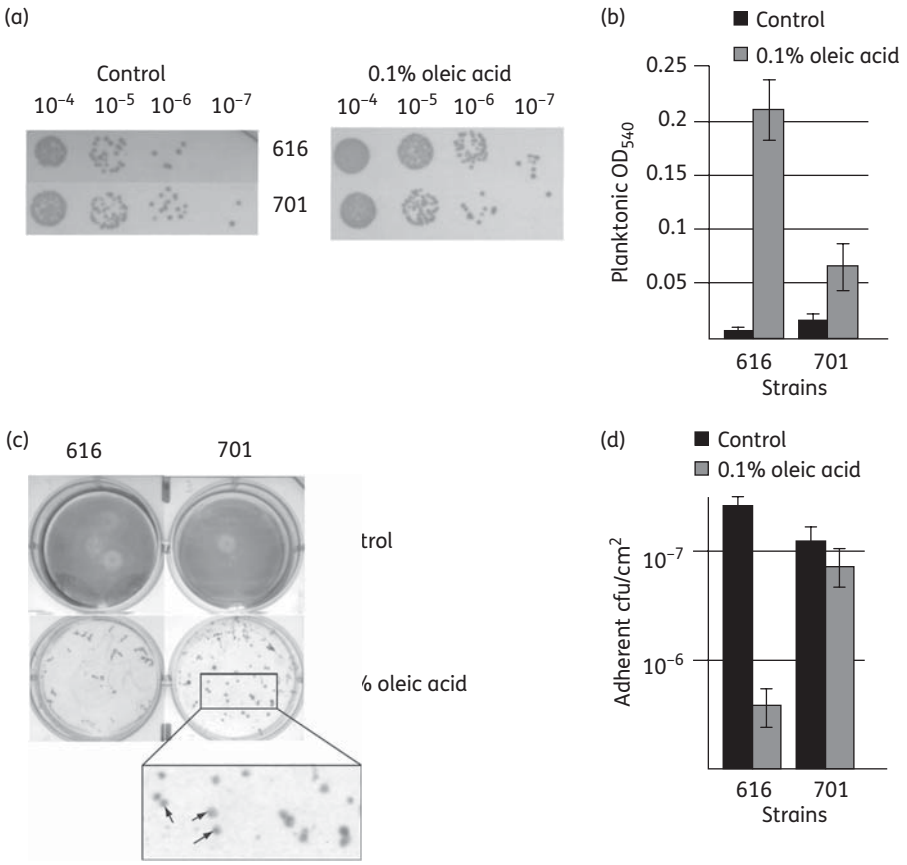

Figure 1. Biofilms of strains 616 and 701 under oleic acid stress and bacterial quantification. (a) Serial dilutions of planktonic cells spotted on agar plates. (b) Quantification of planktonic cells by OD_{540} for two independent experiments. (c) Biofilms stained with crystal violet in a 6-well multititre plate. The box shows a magnification of strain 701 grown in the presence of oleic acid and the arrows show spots stained with crystal violet. (d) Adherence in the presence of oleic acid during two independent experiments. Error bars show the range of duplicate experiments.

shown). Further analyses of the genome content of strain 616 versus strain 701 showed that the two isolates belonged to the same cluster and were most similar to the N315/Mu50 lineage.[32,38] Note also that strains COL, USA300 and NCTC 8325, belonging to clonal complex 8, segregated into the same cluster, as did the two CC1 isolates, MW2 and MSSA476 (Figure 2). Interestingly, the comparison of the 616–701 DAP^S/DAP^R strain pair confirmed the acquisition of genes belonging to pUSA300, underscoring the notion that genetic elements may be acquired *in vivo*.[36] However, on a more global basis, the list of regions or probes showing divergence following 'genomotyping' analysis software (GACK)[46] after hybridization of genomic DNA revealed only a limited number of putative hits when the strain pair isolates were compared. Our microarray design allowed mapping of the *S. aureus* genome using an average of one probe every 450 nucleotides (Table 2).

In addition, given the known major role of the global regulon, *agr*, in staphylococcal virulence factor expression, biofilm formation, persistent bacteraemia and glycopeptide resistance,[47–51] the entire *agr* locus was sequenced in the two principal study strains. Both isolates revealed *agr* locus sequences identical to that of strain Mu3, i.e. with silent point mutations in *agrA* (A→G at position 264; data not shown).

Transcriptomic analysis

The results summarized in Table 3 were obtained from the average values of three independent replicate experiments showing at least a difference of ±1.5-fold between the DAP^S and DAP^R strains. In general, when comparing strain 616 with strain 701, although often statistically significant, most of the fold change values observed for the differentially expressed genes were moderate (2–4-fold range). The total number of genes showing differential expression at 5 h (late exponential phase) was ∼120. For the majority of these genes, the trends in differential expression seen at 5 h were also observed at 3 h (early exponential phase; data not shown). Overall, among these differentially expressed genes, 42% were up-regulated in the DAP^R strain as compared with the DAP^S strain, while 58% were down-regulated. Genes involved in metabolic functions constituted nearly one-half (47%) of those differentially expressed (e.g. sugar metabolism, such as *lac A-B-D-E-F*, or amino acid metabolism, such as *arcA-B-B1-B2-D* or *argF-H* for ornithine degradation and pH homeostasis). Among this category of genes, 74% were up-regulated in the DAP^R isolate as compared with the DAP^S isolate, whereas 26% showed the opposite trend. In addition, ∼15% of the differentially regulated genes belonged to gene families involved in the processes of translation or transcription, with 38% down-regulated and 62% up-regulated in the DAP^R strain versus the DAP^S strain. Cell wall metabolism genes also appeared as an important category distinguishing the two strains, showing only up-regulated genes in the DAP^R isolate (n=9/9). Genes that were 'highly up-regulated' (i.e. ≥5-fold) in the DAP^R strain as compared with the DAP^S strain were observed in the following categories: (i) metabolic functions, such as the *tre* and *lac* operons (>10-fold); (ii) putative

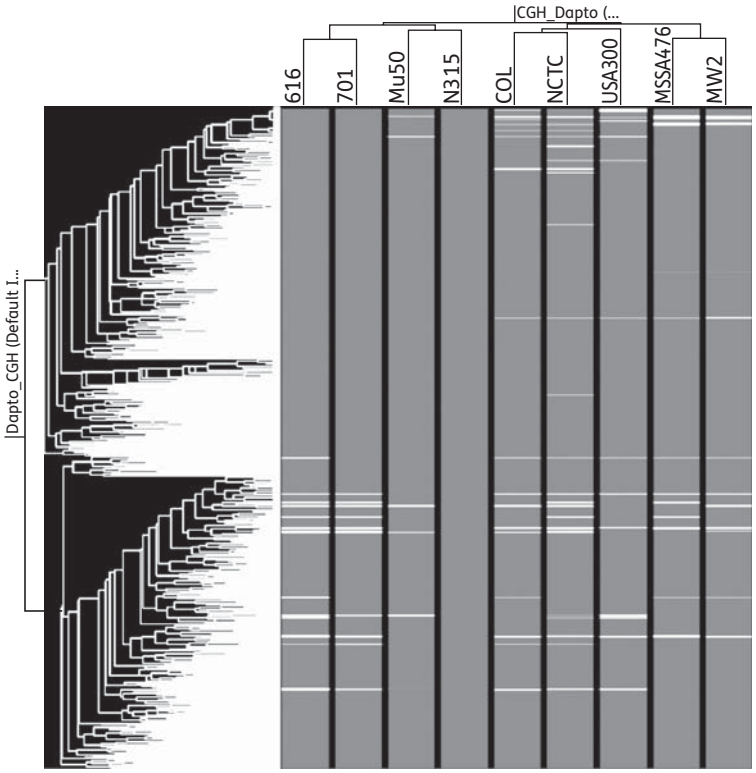

Figure 2. Molecular genotyping of the set of strains. Genotyping tree obtained using microarray covering whole *S. aureus* genomes of eight sequenced strains revealed that our isolates are genetically comparable while N315 appears as the more related reference strain. Each probe is represented by a single row of grey-scaled boxes and each sample corresponds to a single column. The grey areas correspond to genes present, whereas white bars indicate missing genes (N315 used as the reference). The dendrogram (top and left part of the figure) represents the similarity matrix of probe sets.

Table 2. List of genes responsible for difference during complete genome hybridization

Gene	Present only in strain
arsB	701
ccrB	701
ileS	701
nes	701
qacR	701
repA	701
SA1763	701
SA1824	701
SACOL0332	701
SACOL0902	701
SACOL1582	701
SAUSA300_pUSA030027	701
SAUSA300_pUSA030030	701
SAUSA300_pUSA030034	701
SAUSA300_pUSA030035	701
SAUSA300_pUSA030036	701
tnpF	616
traA	701
traB	701
traC	701
traI	701
traJ	701
traK	701
traM	701

virulence factors, such as the *egc* cluster encoding clinically important enterotoxins (>5-fold), *hlb* (>6-fold) and von Willebrand factor-binding protein (MW 766 kDa; >7-fold); and (iii) several ABC transporters (>5-fold). Selected gene grouping differences are further detailed below.

Metabolism and cell wall-related genes

The main categories of metabolic genes that were found to be differentially regulated are involved in the transport of amino acids, carbohydrates, coenzymes and lipids. The vast majority of these genes belonged to amino acid metabolism and transport families (e.g. arginine and ornithine metabolism), and were generally down-regulated by 2–4-fold in the DAP^R versus DAP^S strains. Of note, most of the *lac* operon appeared to be up-regulated in the DAP^R isolate.

Among the genes involved in the biogenesis of the bacterial cell wall, some components of the *lyt* operon (e.g. *lytN and lytH*) were up-regulated in DAP^R versus DAP^S isolates. The *tag* genes (*tagA* and *tagG*) involved in the biogenesis and transport of teichoic acids were found to be significantly up-regulated in the DAP^R isolate. A similar observation was noted for penicillin-binding proteins, *pbp2* and *pbp4*. Moreover, genes belonging to the *yycG/yycF* operon (*yycI* and *yycJ*) were found to be moderately up-regulated in the DAP^R strain. This system has been described as an important regulator of virulence (through the alteration of *ssaA* and *lytM* expression), as well as cell wall biosynthesis (through its action on *tagA-D* expression) and biofilm production. Interestingly, *yycG* has been linked to the DAP^R phenotype in a recent report on such mutants obtained from *in vitro* passages and also following daptomycin exposure *in vivo*.[52,53]

Regulators and virulence factors

Numerous regulatory genes were found to be differentially expressed between the DAP^R and DAP^S strains. Two specific examples were components of the *agr* locus (as well as the downstream *hld* locus responsible for δ-haemolysin production) and the two-component regulatory system, *saeRS*. There were notable trends towards down-regulation of these loci in the DAP^R versus DAP^S strains. Consequently, differential expression of numerous virulence factors that are either *agr*-regulated and/or *saeRS*-regulated was also observed, i.e. *spa*, *fnbA/B*, *hla* and *coa*.[54]

qRT–PCR validation of microarray data for selected genes: comparisons with other DAP^S–DAP^R strain pairs

As an independent, but complementary metric, we utilized qRT–PCR to validate the relative expression levels of selected genes, including several found to be differentially regulated by microarray analysis. This list of genes was specifically prioritized by virtue of known or expected effects on virulence,[17,24] as well as their potential for being part of an interactive regulatory network involved in the DAP^R phenotype [e.g. *agr*; *mprF* (*fmtC*)].[24,55] As previously established by a number of other studies, the absolute magnitude of the normalized amplification signals reflected a broader dynamic range in qRT–PCR as compared with microarray measurements.[32,56]

Overall, the results of the qRT–PCR analyses (Table 4) paralleled the microarray determinations in terms of up- or down-regulation, except for the down-regulated expression of *yycI* in 701. Importantly, qRT–PCR data confirmed the substantial down-regulation of *agr* and *hld* expression in the principal DAP^R versus the DAP^S strain pair, as also detected by microarray analysis. Similarly, a significant increase in the expression of *rot* and *hla* as well as *sarT* and *saeRS* was noted by qRT–PCR comparing the DAP^R versus DAP^S strains, in agreement with the microarray data. However, there was an apparent disconnection between *hla* abundance when compared with *agrA* expression. In strain 701, the low level of *agrA* (activator of *hla*) and the high level of *rot* (repressor of *hla*) transcripts would not normally be compatible with high *hla* transcription. This observation suggests either a mutation/dysfunction in Rot and/or a mutation in the promoter region of *hla*. Alternatively, the increased *hla* may be explained by the increase in SaeRS, increased MgrA and increased SarZ (data not shown). They all increase *hla* even in the absence of RNAIII that acts upon Rot (Figure S2, available as Supplementary data at *JAC* Online, shows some of the potential regulator interactions). Lastly, the levels of *asp23*, *sarA* and *mprF* (*fmtC*) transcription were significantly elevated in comparing the 616–701 DAP^S versus DAP^R isolates, while those for *asp23* and *sarA* were only slightly increased in the DAP^R strain.

We compared the qRT–PCR profiles of the prioritized genes of interest above for our prototype strain pair (616–701) with those of two other recent clinical DAP^S–DAP^R strain pairs (BOY755–BOY300; and MRSA11-11–REF2145) (Table 4). Of note, the

Table 3. List of genes showing differential expression between daptomycin-susceptible and -non-susceptible isolates

Gene	Function	Fold change 701 versus wild-type (5 h)	COG functional category
Transport and metabolism			
arcA	arginine deiminase	0.518	E
arcB	ornithine carbamoyltransferase	0.456	E
arcB1	ornithine carbamoyltransferase	0.415	E
arcB2	ornithine carbamoyltransferase	0.552	E
arcD	arginine/ornithine antiporter	2.037	E
arg	arginase	0.466	E
argF	ornithine carbamoyltransferase	0.448	E
argH	argininosuccinate lyase	4.777	E
SACOL0408	glyoxalase family protein	2.032	E
SACOL1916	amino acid ABC transporter, permease/substrate-binding protein	10.621	E
SAV2440	similar to amino acid permease	2.057	E
lacA	galactose-6-phosphate isomerase subunit LacA	12.630	G
lacB	galactose-6-phosphate isomerase subunit LacB	11.730	G
lacD	tagatose 1,6-diphosphate aldolase	10.539	G
lacE	PTS system, lactose-specific IIBC component	7.762	G
lacF	PTS system, lactose-specific IIA component	7.590	
lacG	6-phospho-β-galactosidase	8.629	
lldP2	l-lactate permease	2.052	C
manA	mannose-6-phosphate isomerase	4.969	G
SA0208	maltose ABC transporter, permease protein	2.642	G
scrA	PTS system lactose-specific IIBC component	7.931	G
tagG	teichoic acid ABC transporter permease protein	1.625	G
treP	phosphoenolpyruvate and trehalose-specific PTS enzyme II	18.050	G
treC	α-amylase family protein	19.550	
SAV0734	FecCD transport family protein	3.969	P
SAV2417	cation efflux family protein	4.536	P
MW0149	hypothetical protein	10.694	I
sirC	putative siderophore transport system permease	9.215	P
fadB	3-hydroxyacyl-CoA dehydrogenase	4.310	I
Cell wall/membrane/envelope biogenesis			
capB	capsular polysaccharide biosynthesis protein CapB	1.788	D
capC	capsular polysaccharide biosynthesis protein CapC	2.433	G
lytN	cell wall hydrolase	3.915	
lytH	*N*-acetylmuramoyl-l-alanine amidase	2.139	M
pbp2	penicillin binding protein 2	1.528	M
pbp4	penicillin binding protein 4	1.841	M
sgtA	transglycosylase domain protein	3.477	M
tagA	teichoic acid ABC transporter permease protein	3.516	M
tagG	teichoic acid ABC transporter permease protein	2.232	
Defence mechanisms and virulence factors			
SACOL2356	ABC transporter, ATP-binding protein	11.740	V
SAV0198	ABC transporter, ATP-binding protein	3.895	V
SAV2360	ABC transporter, permease protein	7.640	V
coa	coagulase precursor	7.618	
fnbB	fibronectin binding protein B	23.575	
SAV0812	similar to secreted von Willebrand factor-binding protein	7.469	
SAV0945	secreted von Willebrand factor-binding protein	10.824	P
sdrC	SdrC protein	1.645	
seg	enterotoxin SEG	5.043	
sei	enterotoxin SEI	5.427	

Continued

Table 3. *Continued*

Gene	Function	Fold change 701 versus wild-type (5 h)	COG functional category
sem	enterotoxin SEM	4.349	
seo	enterotoxin SEO	10.160	
sep	enterotoxin SEP	3.616	
pls	methicillin-resistant surface protein	10.950	
clpL	ATP-dependent Clp protease	0.610	O
hla	α-haemolysin precursor	1.470	
hlb	β-haemolysin	6.584	
hld	δ-haemolysin	0.243	
hlgC	γ-haemolysin	2.087	
Signal transduction mechanisms			
agrA	accessory gene regulator A	0.634	K
agrB	accessory gene regulator B	0.625	O
agrD	accessory gene regulator D	0.574	
saeR	DNA-binding response regulator SaeR	1.966	T
saeS	sensor histidine kinase SaeS	1.856	T
vraR	DNA-binding response regulator VraR	2.219	T
vraS	sensor histidine kinase VraS	2.071	T
lytR	autolysin response regulator protein	4.424	K
rot	repressor of toxins Rot	1.793	
sarT	staphylococcal accessory regulator T	4.177	K
treR	transcriptional regulator, GntR family	10.891	K
Uncharacterized			
SACOL0739/SA0634	acetyltransferase, GNAT family	7.287	J
MW0047	hypothetical protein	3.014	
MW0203/SACOL0206	hypothetical protein	5.728	
MW0372	hypothetical protein	9.550	
MW0638/SACOL0736/SA0631	acetyltransferase, GNAT family	5.764	
SACOL0478/SA0393	superantigen-like protein	6.094	
SACOL1656/SA1428	hypothetical protein	4.880	
SAV0868	hypothetical protein	15.320	
ywpF/SACOL2090/SA1900	ywpF protein	2.080	
yycI/SACOL0022/SA0020	yycI protein	1.675	S
yycJ/SACOL0023/SA0021	metallo-β-lactamase yycJ protein	1.735	R
Various			
SAV2513/SACOL2522/SA2301	DedA family protein	4.169	S
spsA/SACOL0968/SA0825	signal peptidase IA	3.539	U
SACOL0872/SA0755	OsmC/Ohr family protein	0.444	O
rnhC/SACOL1150/SA0987	ribonuclease HIII	5.306	L

COG (cluster of orthologous groups) categories are: C, energy production and conversion; D, cell division and chromosome partitioning; E, amino acid transport and metabolism; G, carbohydrate transport and metabolism; I, lipid metabolism; J, translation, ribosomal structure and biogenesis; K, transcription; L, DNA replication, recombination and repair; M, cell envelope biogenesis, outer membrane; O, post-translational modification, protein turnover, chaperones; P, inorganic ion transport and metabolism; R, general function prediction; S, function unknown; T, signal transduction mechanisms; U, secretion; V, defence mechanism; PTS, phosphotransferase system. Values <1 correspond to downregulated genes.

differential expression profiles for *rot*, *sarS* and *yycF* were quite consistent across the three strain sets, although the net profiles differed significantly among the other genes queried. These data suggested a strong strain-dependent impact on the overall specific genetic networks responsible for the ultimate DAP^R phenotype. These findings are similar to distinct strain-to-strain expression profiling analyses among diverse vancomycin-intermediate *S. aureus* (VISA) strains of *S. aureus*.[13,57,58]

Table 4. Expression of selected genes in each DAP^R from our three strain pairs, and comparison with quantitative transcriptomics and proteomics

	RQ DAP^R versus DAP^S	*rot*	*sarA*	*sarS*	*sarT*	*hla*	*agrA*	*mprF* (*fmtC*)	*asp23*	*hld*	*sarR*	*yycF*	*yycI*	*saeRS*
	BOY300	1.37*	0.92	1.28	0.78	1.00	1.28*	1.12	0.53	1.49*	1.00	0.79*	1.27*	1.66*
	REF2145	1.29*	1.00	1.05	0.77	0.06*	0.58*	0.71*	0.94	0.86	1.04	0.66*	0.72*	0.24*
qRT–PCR	701	2.53*	1.09	1.84*	6.01*	1.82*	0.25*	1.47*	1.49	0.04*	0.74*	0.81*	0.79*	2.84*
Microarray results		1.90	—	—	4.20	1.50	0.63	—	—	0.24	—	—	1.67	2.00
Proteomic results		—	1.4	—	—	—	—	—	2.2*	—	—	—	—	1.00

*Statistically significant (*t*-test value <0.01); RQ, relative quantity.

Quantitative proteomics analysis

Three independent replicates (PR1, PR2 and PR3) identified 771 individual proteins (Figure S3a, available as Supplementary data at *JAC* Online) by combining all proteins identified at least once (see Table S1, available as Supplementary data at *JAC* Online). More than 30% of the identified proteins had more than one predicted transmembrane segment; on average, four to five peptides were identified per protein, confirming the robustness of the quantitative results. To further enhance the accuracy, relative quantification was performed on 546 proteins commonly identified in at least two measurements. Overall, the number of proteins identified in at least two replicates reached >70%, also supporting the robustness of the analysis for the most abundant proteins. Figure S3(b) (available as Supplementary data at *JAC* Online) shows the proportion of proteins in each cluster of orthologous groups (COG) considering the annotation of N315 genome and in our study. Both profiles appear similar except for one category, 'J' (consisting of translation, ribosomal structure and biogenesis), which covers the most abundant bacterial proteins.

Following our conservative quantitative proteomic analysis, only 27 proteins were found to be differentially produced between the DAP^R and DAP^S strains (Table 5). Thus, comparison of this relatively short list with the more extensive differential microarray results failed to detect significant overlap, as is often observed for such analysis.[59,60] Moreover, a number of proteins homologous to those involved in RNA turnover (degradosome) in *Bacillus subtilis* were overexpressed in strain 701, offering a potential explanation for the above lack of overlap between 'omics' techniques.[61] Thus, Eno, RNaseJ1, RNAseJ2, PfkA and Pnp exhibited 1.76-, 1.31-, 1.21-, 1.47- and 1.12-fold increases in the DAP^R strain (Table 5 and Table S1), likely increasing RNA degradation.

After strategic categorization, the ascribed functions of genes or proteins found to be differentially abundant were quite similar. The main protein categories that overlapped with microarray analyses represented target genes involved in membrane metabolism (across all metabolic categories) as well as putative virulence genes (PurH, PsaA, enolase or GapA), stress response genes or genes involved in biofilm formation (MsmX, FabF, enolase, PurH, SdhA-B or Asp23).[41,62,63] Extensive query of the SAMMD database (http://www.bioinformatics.org/sammd/) found that the majority of the protein set (92%) showing differential abundance between our two principal strains has been previously documented to be involved in stress response at the transcriptional level.[64–66] We also found that 13 of the differentially produced proteins (48%) are involved in biofilm regulation,[67–69] such as SdhA-B. Additionally, an important number of proteins appearing in this list (n=12; 44%) are involved in translation processes (COG J).

Discussion

S. aureus (especially MRSA) has been considered for decades as a prototypic hospital-acquired pathogen. However, secular trends have demonstrated that MRSA strains are now responsible for many severe community-acquired infections.[70,71] *S. aureus* has a propensity to rapidly develop resistance to many antimicrobial classes[22,72–76] and this predominantly occurs by: (i) acquisition of resistance determinants;[77] (ii) phenotypic variation;[78] or (iii) profound alterations of its genetic repertoire.[79] This latter category is likely the most difficult to study, as it requires the deployment of extensive and parallel analytical methods (e.g. whole transcriptomic and quantitative proteomic profiling) to uncover discrete genome-scale modifications potentially involved in a given resistance mechanism.[13,14,16,80] In addition, only limited correlations have been reported between a given gene transcript level and the abundance of its respective encoded protein.[59,60] With these issues in mind, our group has recently used several robust analytical approaches to document differential protein abundance between isogenic MRSA strains and their spontaneous glycopeptide-intermediate *S. aureus* (GISA) derivatives.[38] Moreover, we have used such strategies to identify targets involved in cell wall biogenesis or in cell division that were not decipherable by transcriptomic analysis.[59,81] The current study extends these approaches to analyse potential genotypic and phenotypic mechanisms underlying the DAP^R phenotype.

The spontaneous emergence of *S. aureus* with decreased susceptibility to daptomycin can be rapidly obtained *in vitro*,[82] suggesting an early adaptive mechanism(s) induced by exposure to daptomycin. Cui *et al.*[83] reported a correlation between co-evolution of the DAP^R and GISA phenotypes in *S. aureus* by *in vitro* passage in daptomycin-containing environments, suggesting that resistance to these two structurally distinct molecules was triggered by a common pathway(s). More recently, the same group identified putative pathways associated with DAP^R using a transcriptomic approach, highlighting the potential contribution of the *vraSR* two-component regulatory system in this phenotype.[17]

Despite these interesting findings, fundamental insights remain to be identified regarding potential genetic mechanisms

Table 5. Proteins differentially expressed between 701 and 616

Fold change DAP^R versus DAP^S	Description	Common name	Gene name
	METABOLISM		
	energy production and conversion C		
1.62	acetate kinase	AckA	SA1533
0.59	succinate dehydrogenase flavoprotein subunit	SdhA	SA0995
0.61	succinate dehydrogenase iron–sulphur protein subunit	SdhB	SA0996
	carbohydrate transport and metabolism G		
1.76	enolase (2-phosphoglycerate dehydratase)	Eno	SA0731
2.17	glyceraldehyde-3-phosphate dehydrogenase 1	GapA	SA0727
0.36	maltose transmembrane transporter activity		SA0207
0.44	multiple sugar-binding transport ATP-binding protein	MsmX	SA0206
	amino acid transport and metabolism E		
1.54	bifunctional purine biosynthesis protein	PurH	SA0925
	lipid transport and metabolism I		
2.10	3-oxoacyl-(acyl-carrier-protein) synthase 2	FabF	SA0843
	secondary metabolites biosynthesis, transport and catabolism Q		
0.40	dehydrosqualene desaturase	CrtN	SA2348
	inorganic ion transport and metabolism P		
0.56	lipoprotein similar to streptococcal adhesin PsaA		SA0587
	INFORMATION STORAGE AND PROCESSING		
	translation, ribosomal structure and biogenesis J		
1.80	30S ribosomal protein S10	RpsJ	SA2048
1.81	30S ribosomal protein S13	RpsM	SA2025
1.72	30S ribosomal protein S2	RpsB	SA1099
2.52	30S ribosomal protein S3	RpsC	SA2041
1.68	30S ribosomal protein S4	RpsD	SAS052
1.71	30S ribosomal protein S5	RpsE	SA2031
2.08	30S ribosomal protein S6	RpsF	SA0352
1.88	30S ribosomal protein S7	RpsG	SA0504
1.51	50S ribosomal protein L7/L12	RplL	SA0498
1.63	elongation factor Tu (EF-Tu)	TufA	SA0506
1.56	lysyl-tRNA synthetase	LysRS	SA0475
1.71	prolyl-tRNA synthetase	ProRS	SA1106
	CELLULAR PROCESS AND SIGNALLING		
	signal transduction mechanisms T		
0.44	stress response protein		SA1528
	UNKNOWN		
2.18	alkaline shock protein 23	Asp23	SA1984
1.64	GTP-sensing transcriptional pleiotropic repressor	CodY	SA1098
0.54	hypothetical protein		SA0269

of DAP^R in strains that were directly isolated from daptomycin-treated patients. Thus, in the current investigation, we used one principal pair of isolates obtained from a patient with endocarditis, in which the initially DAP^S strain (616) emerged with a DAP^R phenotype (701) during daptomycin treatment.[22] Two additional pairs of isolates showing similar evolution (also obtained from patients with endocarditis), which evolved from DAP^S parental strains during daptomycin therapy, were used in qRT–PCR experiments to evaluate whether or not putative regulatory events leading to DAP^R in *S. aureus* were strain-dependent or more universal.

A number of pivotal and interesting findings emerged from our complementary analytical strategies, which revealed specific changes in gene expression or protein abundance between the DAP^R and DAP^S isolates. Firstly, genomic analysis revealed the presence of the plasmid pUSA300 in the principal DAP^R strain, but not in the DAP^S parental strain. Of note, USA300 clinical isolates, which carry this plasmid, are DAP^S.[36] Thus, the presence of the pUSA300 plasmid does not appear to directly confer the DAP^R phenotype.

Secondly, extensive differences in the expression of several central metabolic function genes were observed in the DAP^S versus DAP^R strains, along with the differential expression of

numerous genes involved in important regulatory processes. For example, the *agr* locus appears to be involved in the DAP^R mechanism. Evidence for this interpretation comes from RNAIII and *hld* transcripts showing moderate decreases, as corroborated by reduced δ-haemolysin production in two of the three DAP^R isolates queried (Figure S1). Simultaneously, we observed increased *saeRS* expression in the DAP^R strain, a finding also compatible with reduced *agr* function.[84] Moreover, expression of *vraSR*, a key two-component regulatory system involved in the control of cell wall synthesis in *S. aureus*, was enhanced in the DAP^R strain. This latter profile has been previously identified in GISA isolates[14] and in strains exposed to daptomycin *in vitro*.[85] We also noticed a slight increase of the *asp23* transcript levels and its real increase at the protein level in the DAP^R; this locus is a reliable surrogate marker for expression of the key global regulator, SigB.[86] Collectively, these observations are consistent with a recent report showing that daptomycin impacts genes involved in both the cell wall stress stimulon and in membrane depolarization.[85]

Thirdly, the notion that daptomycin can target the staphylococcal cell wall as well as its CM was underscored in the evolution towards DAP^R. Thus, the abundance of differentially expressed genes (as well as their translation products) involved in the metabolism of the bacterial cell wall was notably distinct between the principal strain pair. A number of such genes (e.g. *pbp2* and *pbp4*, *lytN* and *lytH*, *tagA*, and *sgtA*) have been previously reported to be differentially regulated in the following conditions: stress response to cell wall-active antibiotics;[87] mild acidic shock;[88] or during the stringent response.[64] Likewise, our recent findings of thickened cell walls in this same DAP^R strain (701) by TEM,[25] as well as in an *in vitro*-selected DAP^R strain are also consistent with this paradigm.[8,13] Current studies in our laboratories are focused upon a detailed comparative evaluation of the cell wall compositions of our DAP^S–DAP^R strain pair.[25]

Fourthly, we employed qRT–PCR to confirm the differential expression profiles of a number of critical *S. aureus* global regulators and structural virulence genes that were disclosed in the transcriptomic analyses. The specific genes assessed by qRT–PCR were selected based on their putative roles in endovascular infections (related to their individual or combined impacts upon surface adhesins, exotoxins and/or exoproteins likely involved in one or more pathogenetic phases of such infections).[89] As in the microarray analyses above, qRT–PCR analysis showed that the expression of most of these genes was up-regulated in the DAP^R strain (701) as compared with the DAP^S parental strain (616), with the notable exceptions of down-regulation of *sarR* and *agr* expression (as evidenced by reductions in both *agrA* and *hld* expression levels). The finding of reduced *agr* expression in the DAP^R strain is of interest in the context of VISA strains. Several studies have confirmed the relationship of *agr* deletions or point mutations, reduced *agr* function phenotypically and glycopeptide resistance.[15] Despite down-regulation of *agr* in strain 701, *hla* expression was significantly up-regulated in the face of *rot* up-regulation. One logical explanation for this seemingly paradoxical interactive network of gene expressions is the acquisition of a loss-in-function mutation in *rot*;[90,91] sequence analysis of the *rot* locus is in progress.

In formulating potential DAP^R interactive pathways, it seems clear that there are strain-to-strain variations. For the 616–701 strain pair, in addition to increased *rot* and reduced *agr* in 701, *sarT* (encoding for a negative regulators of *hla*) is also up-regulated. Thus, increased *hla* production may be explained by the increase in *saeRS*, increased *mgrA* and increased *sarZ* expression (our microarray results showed a trend towards increased expression in 701). Indeed they will all increase *hla* even in the absence of RNAIII acting upon Rot. Hence, we propose that 701 shows increased *hla* even in the presence of Rot and SarT repressor functionalities, i.e. it is either autonomous or SaeRS, MgrA and SarZ are stimulating increased *hla* transcripts.[51] In the 11-11/REF2145 strain pair, reduced *hla* transcript levels in REF2145 are associated with reduced *agr* expression and increased *rot* transcription. However, in BOY300, *hla* transcripts are decreased despite the increase in *agr*, *hld* and *saeRS*, without any increase in *rot* transcripts, suggesting that the production of *hla* has become autonomous. Finally, in terms of *mprF* (*fmtC*) expression involved in *saeRS* regulation,[92] this tends to vary from strain to strain, ranging from unchanged (BOY300), to increased (701), to reduced (REF2145). It has been well chronicled that in daptomycin-resistant staphylococci, mutations in the *mprF* gene usually produce gains in function.[22,24] Thus, it is quite possible that strains BOY300 and REF2145 have reduced transcript levels, but increased activity of MprF due to gain-in-function mutations (regulator interactions are summarized in Figure S2).

Our studies above support a hypothesis that the DAP^R phenotype results from coordination among multiple adaptive response circuits. For example, our observed reduction in *sarR* expression in the DAP^R isolate can be linked to an increase in *sarA* expression. In turn, an increase in *sarA* expression could modify biofilm formation as well as increase *hla* expression via an *agr*-independent pathway.[93] Supporting this concept, the current studies demonstrated a clear difference in biofilm dynamics and phenotype in the DAP^S versus DAP^R strains.

Finally, a pivotal observation in our investigation was that the key regulatory locus, *yycFGHI*, was differentially expressed when our DAP^S and DAP^R strain sets were compared. This operon is a key regulator affecting CM lipid homeostasis, cell wall metabolism and biofilm formation.[19,53,94,95] The expression of this regulator contributes to modification of the net surface charge via both *mprF* and *dlt* pathways; thus, likely impacting daptomycin binding as well as the initial attachment phases in biofilm formation.[19] These latter interpretations are substantiated by our findings that our principal study strain pair (616–701) differed in their capacity to form biofilm in the presence of the antimicrobial lipid, oleic acid. Oleic acid has been reported previously as a microbicidal agent against *S. aureus*, presumably through a mechanism involving membrane fluidity and the lipid composition of the cytoplasmic membrane.[9] We used oleic acid instead of daptomycin, because: (i) they share similarities in their lipid tail (7–8 CH_2 following a CH_3); and (ii) we were able to use similar concentrations of this compound for both strains. Moreover, another chemical compound called friulimicin B that shares similar structure and chemical properties with daptomycin also possesses a lipid tail of 8 CH_2 (+2 CH_3 terminus) before a C=C double bond, like the oleic acid lipid tail.[96] Importantly, like daptomycin, friulimicin B absolutely requires Ca^{2+} for antimicrobial activity. In the present study, the DAP^R isolate retained the ability to produce an abundant and structurally distinct biofilm, with greater adhesive properties, even in the setting

of an antibacterial lipid environment (i.e. oleic acid exposure). It is tempting to speculate that an adaptation to the lipid moiety of daptomycin in DAP^R strains may be involved in the relative resistance of this strain to oleic acid, especially within biofilms. If so, this modification of biofilm formation could be linked to an increase in *sarA* expression in the DAP^R strain. For example, Weiss *et al*.[97] showed an increased susceptibility to daptomycin linked to a decreased biofilm adherence (*in vivo*) in an *S. aureus sarA* mutant.

Examination of our composite data sets from our principal strain pair suggested that changes in YycF and YycI could account for many of the changes found in the DAP^R strain. Increased positive surface charge (e.g. via gain-in-function mutations in *mprF*) and increased membrane fluidity have been associated with DAP^R.[18] In addition, some DAP^R strains show thickened cell walls and altered biofilm formation. Activated YycF positively regulates genes involved in cell division, and ultimately cell wall thickness and division planes. Thus, a reduction in YycF activity due to either increased YycI activity (an inhibitor of YycF) or to a mutation in *yycF* could account for alterations in the cell wall structure. When *yycI* transcripts are increased, then YycFG will have reduced activity (i.e. strain BOY300). When *yycF* is reduced, then there is no need to have higher levels of *yycI*, as either high *yycI* or low *yycF* will result in the same phenotype. This implies that more than one mutation can provide the same phenotype, i.e. reduced YycF∼P. Moreover, YycF regulates *mprF*, as well as MgrA, which is the sole regulator of *sarZ* and a repressor of *sarS* and *sarT*,[98] which are differentially regulated in our three backgrounds (Table 4 and Figure S2). MgrA represses *icaABDC*, which is essential for biofilm formation. Thus, reduced activation of *mgrA* due to decreased YycF activity could result in increased biofilm formation. Lastly, activated YycF is a positive regulator of PhoP, which negatively regulates the *tagA* operon. As TagA is the first committed step in the lipoteichoic acid (LTA) pathway, a reduction in YycF activity would reduce the repressive effect of PhoP, thereby leading to more LTA. LTA inhibits the autolysin (Alt) and increases the positive charge on the cell wall, thereby influencing both cell wall thickness and daptomycin susceptibility, respectively.[8] These interactive paradigms are summarized in a putative network model that allows integration of biofilm formation, changes in positive surface charge, cell wall structure, daptomycin binding and cell wall susceptibility to lipids (Figure 3). We view this model as a working hypothesis upon which future experiments can be performed in the examination of DAP^R. Another explanation for the daptomycin-resistant phenotype would be that there are multiple mutations in distinct regulatory pathways in such strains. This hypothesis is compatible with the stepwise development of resistance that is found both in patients receiving long-term daptomycin, as well as in strains undergoing serial *in vitro* passage in daptomycin in the laboratory (Figure S2). Clearly, not all our data sets fit into a single cohesive model; this observation is entirely consistent with the stepwise development of DAP^R, as well as a summation of multiple mutations producing this resistance phenotype.

It should be emphasized that in comparing qRT–PCR data sets between our three DAP^S–DAP^R strain pairs, there were several consistent observations in the DAP^R strains; up-regulation of *rot* and *sarS*, and down-regulation of *yycF*. However, expression patterns of the other 10 genes queried in our focused analysis yielded no universally consistent profile. This finding would underscore the concepts that: (i) DAP^R networks are complex and strain specific; and (ii) the accumulation of diverse mutations during daptomycin exposures, as confirmed for many reported DAP^R strains,[22] may well be critical in ultimate DAP^R 'pathways'.

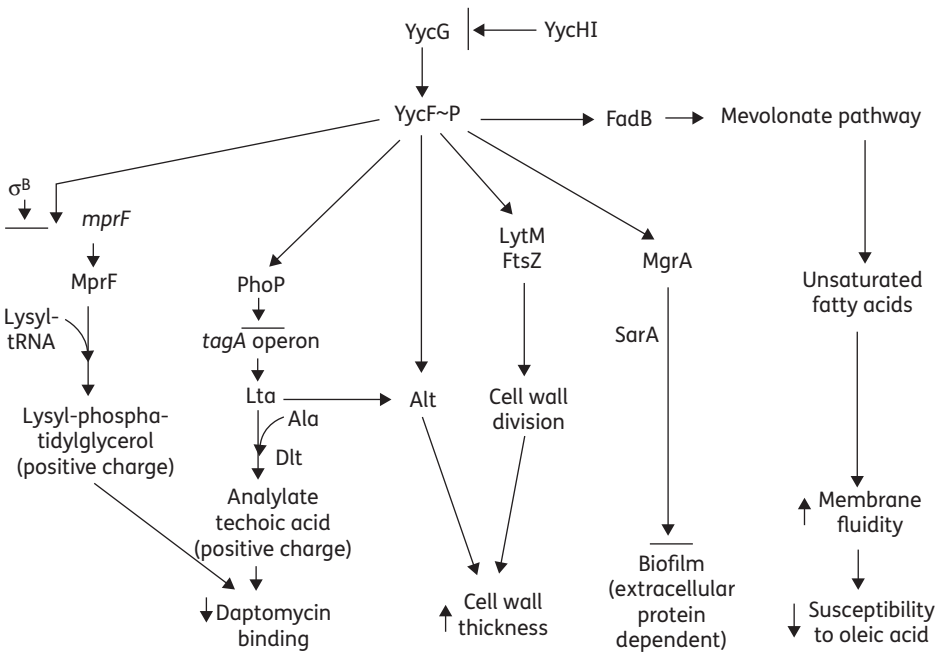

Figure 3. Potential pathways leading to DAP^R. Cell wall metabolism and regulators appear as major targets of mechanisms leading to DAP^R acquired *in vivo* during therapy. The biosynthesis of bacterial envelopes is involved in the process leading to major phenotypic changes between DAP^S and DAP^R *S. aureus*. Black bars represent inhibition.

Conclusions

In vivo emergence of DAP^R in *S. aureus* during daptomycin treatment is the result of multiple adaptations in metabolic functions, global regulatory pathways, as well as the biogenesis of the cellular envelope. The evolution of DAP^R in the clinical strain set 616–701 corresponded with an increase in the DAP^R strain's capability to generate a pronounced and structurally distinct biofilm, and to resist toxic membrane-targeting antimicrobial lipids. Combined transcriptomic and proteomic analyses provided a global view of the complex process corresponding to the adaptive DAP^R phenotype. Several genes and proteins, potentially involved in the emergence of DAP^R *in vivo*, were identified in this study, and appear quite distinct from *in vitro*-selected DAP^R organisms. Finally, comparison between three genotypically distinct strain pairs revealed a strain-dependent, multifactorial regulation in the DAP^R phenotype. It appears likely that the global regulatory locus, *yycFGHI*, plays a key role in the development of DAP^R.

Acknowledgements

We thank Dr Ambrose Cheung (Dartmouth Medical College, Hanover, NH, USA) for assistance in the genotypic interpretations and Dr Andreas Peschel (University of Tubingen, Germany) for many helpful discussions.

Funding

This research was supported by grants from the NIH to A. S. B. (AI-039108) and M. R. Y. (AI-039001), grants 3100A0-112370/1 (to J. S.) and 3100A0-116075 (to P. F.) from the Swiss National Science Foundation.

Transparency declarations

None to declare.

Supplementary data

Figures S1–S3 and Table S1 are available Supplementary data at *JAC* Online (http://jac.oxfordjournals.org/).

References

1 Mortara LA, Bayer AS. *Staphylococcus aureus* bacteremia and endocarditis. New diagnostic and therapeutic concepts. *Infect Dis Clin North Am* 1993; **7**: 53–68.

2 Hobbs JK, Miller K, O'Neill AJ *et al*. Consequences of daptomycin-mediated membrane damage in *Staphylococcus aureus*. *J Antimicrob Chemother* 2008; **62**: 1003–8.

3 Sakoulas G, Eliopoulos GM, Alder J *et al*. Efficacy of daptomycin in experimental endocarditis due to methicillin-resistant *Staphylococcus aureus*. *Antimicrob Agents Chemother* 2003; **47**: 1714–8.

4 Lew DP, Waldvogel FA. Osteomyelitis. *Lancet* 2004; **364**: 369–79.

5 Eliopoulos GM, Thauvin C, Gerson B *et al*. In vitro activity and mechanism of action of A21978C1, a novel cyclic lipopeptide antibiotic. *Antimicrob Agents Chemother* 1985; **27**: 357–62.

6 Gu JQ, Nguyen KT, Gandhi C *et al*. Structural characterization of daptomycin analogues A21978C1-3(d-Asn11) produced by a recombinant *Streptomyces roseosporus* strain. *J Nat Prod* 2007; **70**: 233–40.

7 Lakey JH, Ptak M. Fluorescence indicates a calcium-dependent interaction between the lipopeptide antibiotic LY146032 and phospholipid membranes. *Biochemistry* 1988; **27**: 4639–45.

8 Mishra NN, Yang SJ, Sawa A *et al*. Analysis of cell membrane characteristics of in vitro-selected daptomycin-resistant strains of methicillin-resistant *Staphylococcus aureus*. *Antimicrob Agents Chemother* 2009; **53**: 2312–8.

9 Chamberlain NR, Mehrtens BG, Xiong Z *et al*. Correlation of carotenoid production, decreased membrane fluidity, and resistance to oleic acid killing in *Staphylococcus aureus* 18Z. *Infect Immun* 1991; **59**: 4332–7.

10 Campbell IM, Crozier DN, Pawagi AB. Effect of hypobaric oxygen and oleic acid on respiration of *Staphylococcus aureus*. *Eur J Clin Microbiol* 1986; **5**: 622–8.

11 Stenz L, Francois P, Fischer A *et al*. Impact of oleic acid (cis-9-octadecenoic acid) on bacterial viability and biofilm production in *Staphylococcus aureus*. *FEMS Microbiol Lett* 2008; **287**: 149–55.

12 Gotz F. *Staphylococcus* and biofilms. *Mol Microbiol* 2002; **43**: 1367–78.

13 Cui L, Ma X, Sato K *et al*. Cell wall thickening is a common feature of vancomycin resistance in *Staphylococcus aureus*. *J Clin Microbiol* 2003; **41**: 5–14.

14 Kuroda M, Kuroda H, Oshima T *et al*. Two-component system VraSR positively modulates the regulation of cell-wall biosynthesis pathway in *Staphylococcus aureus*. *Mol Microbiol* 2003; **49**: 807–21.

15 Sakoulas G, Eliopoulos GM, Moellering RC Jr *et al*. Accessory gene regulator (*agr*) locus in geographically diverse *Staphylococcus aureus* isolates with reduced susceptibility to vancomycin. *Antimicrob Agents Chemother* 2002; **46**: 1492–502.

16 Koehl JL, Muthaiyan A, Jayaswal RK *et al*. Cell wall composition and decreased autolytic activity and lysostaphin susceptibility of glycopeptide-intermediate *Staphylococcus aureus*. *Antimicrob Agents Chemother* 2004; **48**: 3749–57.

17 Camargo IL, Neoh HM, Cui L *et al*. Serial daptomycin selection generates daptomycin-nonsusceptible *Staphylococcus aureus* strains with a heterogeneous vancomycin-intermediate phenotype. *Antimicrob Agents Chemother* 2008; **52**: 4289–99.

18 Martin PK, Li T, Sun D *et al*. Role in cell permeability of an essential two-component system in *Staphylococcus aureus*. *J Bacteriol* 1999; **181**: 3666–73.

19 Dubrac S, Boneca IG, Poupel O *et al*. New insights into the WalK/WalR (YycG/YycF) essential signal transduction pathway reveal a major role in controlling cell wall metabolism and biofilm formation in *Staphylococcus aureus*. *J Bacteriol* 2007; **189**: 8257–69.

20 Mwangi MM, Wu SW, Zhou Y *et al*. Tracking the in vivo evolution of multidrug resistance in *Staphylococcus aureus* by whole-genome sequencing. *Proc Natl Acad Sci USA* 2007; **104**: 9451–6.

21 Ohta T, Hirakawa H, Morikawa K *et al*. Nucleotide substitutions in *Staphylococcus aureus* strains, Mu50, Mu3, and N315. *DNA Res* 2004; **11**: 51–6.

22 Jones T, Yeaman MR, Sakoulas G *et al*. Failures in clinical treatment of *Staphylococcus aureus* infection with daptomycin are associated with alterations in surface charge, membrane phospholipid asymmetry, and drug binding. *Antimicrob Agents Chemother* 2008; **52**: 269–78.

23 Ernst CM, Staubitz P, Mishra NN *et al*. The bacterial defensin resistance protein MprF consists of separable domains for lipid lysinylation and antimicrobial peptide repulsion. *PLoS Pathog* 2009; **5**: e1000660.

24 Yang SJ, Xiong YQ, Dunman PM *et al*. Regulation of *mprF* in daptomycin-nonsusceptible *Staphylococcus aureus* strains. *Antimicrob Agents Chemother* 2009; **53**: 2636–7.

25 Yang SJ, Nast CC, Mishra NN *et al*. Cell wall thickening is not a universal accompaniment of the daptomycin nonsusceptibility phenotype in *Staphylococcus aureus*: evidence for multiple resistance mechanisms. *Antimicrob Agents Chemother* 2010; **54**: 3079–85.

26 Yang SJ, Kreiswirth BN, Sakoulas G *et al*. Enhanced expression of *dltABCD* is associated with the development of daptomycin nonsusceptibility in a clinical endocarditis isolate of *Staphylococcus aureus*. *J Infect Dis* 2009; **200**: 1916–20.

27 Murthy MH, Olson ME, Wickert RW *et al*. Daptomycin non-susceptible meticillin-resistant *Staphylococcus aureus* USA 300 isolate. *J Med Microbiol* 2008; **57**: 1036–8.

28 Traber K, Novick R. A slipped-mispairing mutation in AgrA of laboratory strains and clinical isolates results in delayed activation of agr and failure to translate δ- and α-haemolysins. *Mol Microbiol* 2006; **59**: 1519–30.

29 McCalla C, Smyth DS, Robinson DA *et al*. Microbiological and genotypic analysis of methicillin-resistant *Staphylococcus aureus* bacteremia. *Antimicrob Agents Chemother* 2008; **52**: 3441–3.

30 Francois P, Huyghe A, Charbonnier Y *et al*. Use of an automated multiple-locus, variable-number tandem repeat-based method for rapid and high-throughput genotyping of *Staphylococcus aureus* isolates. *J Clin Microbiol* 2005; **43**: 3346–55.

31 Francois P, Harbarth S, Huyghe A *et al*. Methicillin-resistant *Staphylococcus aureus*, Geneva, Switzerland, 1993–2005. *Emerg Infect Dis* 2008; **14**: 304–7.

32 Charbonnier Y, Gettler BM, Francois P *et al*. A generic approach for the design of whole-genome oligoarrays, validated for genomotyping, deletion mapping and gene expression analysis on *Staphylococcus aureus*. *BMC Genomics* 2005; **6**: 95.

33 Kuroda M, Ohta T, Uchiyama I *et al*. Whole genome sequencing of meticillin-resistant *Staphylococcus aureus*. *Lancet* 2001; **357**: 1225–40.

34 Baba T, Takeuchi F, Kuroda M *et al*. Genome and virulence determinants of high virulence community-acquired MRSA. *Lancet* 2002; **359**: 1819–27.

35 Gill SR, Fouts DE, Archer GL *et al*. Insights on evolution of virulence and resistance from the complete genome analysis of an early methicillin-resistant *Staphylococcus aureus* strain and a biofilm-producing methicillin-resistant *Staphylococcus epidermidis* strain. *J Bacteriol* 2005; **187**: 2426–38.

36 Diep BA, Gill SR, Chang RF *et al*. Complete genome sequence of USA300, an epidemic clone of community-acquired meticillin-resistant *Staphylococcus aureus*. *Lancet* 2006; **367**: 731–9.

37 Holden MT, Feil EJ, Lindsay JA *et al*. Complete genomes of two clinical *Staphylococcus aureus* strains: evidence for the rapid evolution of virulence and drug resistance. *Proc Natl Acad Sci USA* 2004; **101**: 9786–91.

38 Scherl A, Francois P, Charbonnier Y *et al*. Exploring glycopeptide resistance in *Staphylococcus aureus*: a combined proteomics and transcriptomics approach for the identification of resistance related markers. *BMC Genomics* 2006; **7**: 296.

39 Talaat AM, Howard ST, Hale W *et al*. Genomic DNA standards for gene expression profiling in *Mycobacterium tuberculosis*. *Nucleic Acids Res* 2002; **30**: e104.

40 Garzoni C, Francois P, Huyghe A *et al*. A global view of *Staphylococcus aureus* whole genome expression upon internalization in human epithelial cells. *BMC Genomics* 2007; **8**: 171.

41 Renzoni A, Francois P, Li D *et al*. Modulation of fibronectin adhesins and other virulence factors in a teicoplanin-resistant derivative of methicillin-resistant *Staphylococcus aureus*. *Antimicrob Agents Chemother* 2004; **48**: 2958–65.

42 Vaezzadeh AR, Simicevic J, Chauvet A *et al*. Imaging mass spectrometry using peptide isoelectric focusing. *Rapid Commun Mass Spectrom* 2008; **22**: 2667–76.

43 Elias JE, Gygi SP. Target–decoy search strategy for increased confidence in large-scale protein identifications by mass spectrometry. *Nat Methods* 2007; **4**: 207–14.

44 Dayon L, Hainard A, Licker V *et al*. Relative quantification of proteins in human cerebrospinal fluids by MS/MS using 6-plex isobaric tags. *Anal Chem* 2008; **80**: 2921–31.

45 Shadforth IP, Dunkley TP, Lilley KS *et al*. i-Tracker: for quantitative proteomics using iTRAQ. *BMC Genomics* 2005; **6**: 145.

46 Kim CC, Joyce EA, Chan K *et al*. Improved analytical methods for microarray-based genome-composition analysis. *Genome Biol* 2002; **3**: 0065.1–0065.17.

47 Dunman PM, Murphy E, Hanney S *et al*. Transcription profiling-based identification of *Staphylococcus aureus* genes regulated by the *agr* and/or *sarA* loci. *J Bacteriol* 2001; **183**: 7341–53.

48 Pantrangi M, Singh VK, Wolz C *et al*. Staphylococcal superantigen-like genes, *ssl5* and *ssl8*, are positively regulated by Sae and negatively by Agr in the Newman strain. *FEMS Microbiol Lett* 2010; **308**: 175–84.

49 Beenken KE, Mrak LN, Griffin LM *et al*. Epistatic relationships between sarA and agr in *Staphylococcus aureus* biofilm formation. *PLoS One* 2010; **5**: e10790.

50 Majerczyk CD, Dunman PM, Luong TT *et al*. Direct targets of CodY in *Staphylococcus aureus*. *J Bacteriol* 2010; **192**: 2861–77.

51 Tamber S, Cheung AL. SarZ promotes the expression of virulence factors and represses biofilm formation by modulating SarA and agr in *Staphylococcus aureus*. *Infect Immun* 2009; **77**: 419–28.

52 Quinn B, Hussain S, Malik M *et al*. Daptomycin inoculum effects and mutant prevention concentration with *Staphylococcus aureus*. *J Antimicrob Chemother* 2007; **60**: 1380–3.

53 Friedman L, Alder JD, Silverman JA. Genetic changes that correlate with reduced susceptibility to daptomycin in *Staphylococcus aureus*. *Antimicrob Agents Chemother* 2006; **50**: 2137–45.

54 Cheung AL, Bayer AS, Zhang G *et al*. Regulation of virulence determinants in vitro and in vivo in *Staphylococcus aureus*. *FEMS Immunol Med Microbiol* 2004; **40**: 1–9.

55 Sakoulas G, Eliopoulos GM, Fowler VG Jr *et al*. Reduced susceptibility of *Staphylococcus aureus* to vancomycin and platelet microbicidal protein correlates with defective autolysis and loss of accessory gene regulator (*agr*) function. *Antimicrob Agents Chemother* 2005; **49**: 2687–92.

56 Ramakrishnan R, Dorris D, Lublinsky A *et al*. An assessment of Motorola CodeLink microarray performance for gene expression profiling applications. *Nucleic Acids Res* 2002; **30**: e30.

57 Wootton M, MacGowan AP, Walsh TR. Expression of *tcaA* and *mprF* and glycopeptide resistance in clinical glycopeptide-intermediate *Staphylococcus aureus* (GISA) and heteroGISA strains. *Biochim Biophys Acta* 2005; **1726**: 326–7.

58 Wootton M, Bennett PM, MacGowan AP *et al*. Strain-specific expression levels of *pbp4* exist in isolates of glycopeptide-intermediate *Staphylococcus aureus* (GISA) and heterogeneous GISA. *Antimicrob Agents Chemother* 2005; **49**: 3598–9.

59 Scherl A, Francois P, Bento M *et al*. Correlation of proteomic and transcriptomic profiles of *Staphylococcus aureus* during the post-exponential phase of growth. *J Microbiol Methods* 2005; **60**: 247–57.

60 Corbin RW, Paliy O, Yang F *et al*. Toward a protein profile of *Escherichia coli*: comparison to its transcription profile. *Proc Natl Acad Sci USA* 2003; **100**: 9232–7.

61 Lehnik-Habrink M, Pfortner H, Rempeters L *et al*. The RNA degradosome in *Bacillus subtilis*: identification of CshA as the major

RNA helicase in the multiprotein complex. *Mol Microbiol* 2010; doi:10.1111/j.1365-2958.2010.07264.x.

62 Conlon KM, Humphreys H, O'Gara JP. Inactivations of *rsbU* and *sarA* by IS256 represent novel mechanisms of biofilm phenotypic variation in *Staphylococcus epidermidis*. *J Bacteriol* 2004; **186**: 6208–19.

63 Goerke C, Esser S, Kummel M *et al*. *Staphylococcus aureus* strain designation by *agr* and *cap* polymorphism typing and delineation of *agr* diversification by sequence analysis. *Int J Med Microbiol* 2005; **295**: 67–75.

64 Anderson KL, Roberts C, Disz T *et al*. Characterization of the *Staphylococcus aureus* heat shock, cold shock, stringent, and SOS responses and their effects on log-phase mRNA turnover. *J Bacteriol* 2006; **188**: 6739–56.

65 Schlag S, Nerz C, Birkenstock TA *et al*. Inhibition of staphylococcal biofilm formation by nitrite. *J Bacteriol* 2007; **189**: 7911–9.

66 Richardson AR, Dunman PM, Fang FC. The nitrosative stress response of *Staphylococcus aureus* is required for resistance to innate immunity. *Mol Microbiol* 2006; **61**: 927–39.

67 Brady RA, Leid JG, Camper AK *et al*. Identification of *Staphylococcus aureus* proteins recognized by the antibody-mediated immune response to a biofilm infection. *Infect Immun* 2006; **74**: 3415–26.

68 Beenken KE, Dunman PM, McAleese F *et al*. Global gene expression in *Staphylococcus aureus* biofilms. *J Bacteriol* 2004; **186**: 4665–84.

69 Resch A, Rosenstein R, Nerz C *et al*. Differential gene expression profiling of *Staphylococcus aureus* cultivated under biofilm and planktonic conditions. *Appl Environ Microbiol* 2005; **71**: 2663–76.

70 Chambers HF. The changing epidemiology of *Staphylococcus aureus*? *Emerg Infect Dis* 2001; **7**: 178–82.

71 Charlebois ED, Perdreau-Remington F, Kreiswirth B *et al*. Origins of community strains of methicillin-resistant *Staphylococcus aureus*. *Clin Infect Dis* 2004; **39**: 47–54.

72 Barber M. Methicillin-resistant staphylococci. *J Clin Pathol* 1961; **14**: 385–93.

73 Chang S, Sievert DM, Hageman JC *et al*. Infection with vancomycin-resistant *Staphylococcus aureus* containing the *vanA* resistance gene. *N Engl J Med* 2003; **348**: 1342–7.

74 Hiramatsu K, Okuma K, Ma XX *et al*. New trends in *Staphylococcus aureus* infections: glycopeptide resistance in hospital and methicillin resistance in the community. *Curr Opin Infect Dis* 2002; **15**: 407–13.

75 Cambau E, Gutmann L. Mechanisms of resistance to quinolones. *Drugs* 1993; **45** Suppl 3: 15–23.

76 Tsiodras S, Gold HS, Sakoulas G *et al*. Linezolid resistance in a clinical isolate of *Staphylococcus aureus*. *Lancet* 2001; **358**: 207–8.

77 Ryffel C, Kayser FH, Berger-Bachi B. Correlation between regulation of *mecA* transcription and expression of methicillin resistance in staphylococci. *Antimicrob Agents Chemother* 1992; **36**: 25–31.

78 Proctor RA, Kahl B, von Eiff C *et al*. Staphylococcal small colony variants have novel mechanisms for antibiotic resistance. *Clin Infect Dis* 1998; **27** Suppl 1: S68–74.

79 Hiramatsu K. Vancomycin-resistant *Staphylococcus aureus*: a new model of antibiotic resistance. *Lancet Infect Dis* 2001; **1**: 147–55.

80 Boyle-Vavra S, Carey RB, Daum RS. Development of vancomycin and lysostaphin resistance in a methicillin-resistant *Staphylococcus aureus* isolate. *J Antimicrob Chemother* 2001; **48**: 617–25.

81 Cui L, Lian JQ, Neoh HM *et al*. DNA microarray-based identification of genes associated with glycopeptide resistance in *Staphylococcus aureus*. *Antimicrob Agents Chemother* 2005; **49**: 3404–13.

82 Liebowitz LD, Saunders J, Chalkley LJ *et al*. In vitro selection of bacteria resistant to LY146032, a new cyclic lipopeptide. *Antimicrob Agents Chemother* 1988; **32**: 24–6.

83 Cui L, Tominaga E, Neoh HM *et al*. Correlation between reduced daptomycin susceptibility and vancomycin resistance in vancomycin-intermediate *Staphylococcus aureus*. *Antimicrob Agents Chemother* 2006; **50**: 1079–82.

84 Rose WE, Rybak MJ, Tsuji BT *et al*. Correlation of vancomycin and daptomycin susceptibility in *Staphylococcus aureus* in reference to accessory gene regulator (*agr*) polymorphism and function. *J Antimicrob Chemother* 2007; **59**: 1190–3.

85 Muthaiyan A, Silverman JA, Jayaswal RK *et al*. Transcriptional profiling reveals that daptomycin induces the *Staphylococcus aureus* cell wall stress stimulon and genes responsive to membrane depolarization. *Antimicrob Agents Chemother* 2008; **52**: 980–90.

86 Mongodin E, Finan J, Climo MW *et al*. Microarray transcription analysis of clinical *Staphylococcus aureus* isolates resistant to vancomycin. *J Bacteriol* 2003; **185**: 4638–43.

87 Utaida S, Dunman PM, Macapagal D *et al*. Genome-wide transcriptional profiling of the response of *Staphylococcus aureus* to cell-wall-active antibiotics reveals a cell-wall-stress stimulon. *Microbiology* 2003; **149**: 2719–32.

88 Weinrick B, Dunman PM, McAleese F *et al*. Effect of mild acid on gene expression in *Staphylococcus aureus*. *J Bacteriol* 2004; **186**: 8407–23.

89 Lowy FD. *Staphylococcus aureus* infections. *N Engl J Med* 1998; **339**: 520–32.

90 Geisinger E, Adhikari RP, Jin R *et al*. Inhibition of *rot* translation by RNAIII, a key feature of *agr* function. *Mol Microbiol* 2006; **61**: 1038–48.

91 Goerke C, Fluckiger U, Steinhuber A *et al*. Impact of the regulatory loci *agr*, *sarA* and *sae* of *Staphylococcus aureus* on the induction of α-toxin during device-related infection resolved by direct quantitative transcript analysis. *Mol Microbiol* 2001; **40**: 1439–47.

92 Sievers S, Ernst CM, Geiger T *et al*. Changing the phospholipid composition of *Staphylococcus aureus* causes distinct changes in membrane proteome and membrane-sensory regulators. *Proteomics* 2010; **10**: 1685–93.

93 Chien Y, Manna AC, Projan SJ *et al*. SarA, a global regulator of virulence determinants in *Staphylococcus aureus*, binds to a conserved motif essential for *sar*-dependent gene regulation. *J Biol Chem* 1999; **274**: 37169–76.

94 Dubrac S, Msadek T. Identification of genes controlled by the essential YycG/YycF two-component system of *Staphylococcus aureus*. *J Bacteriol* 2004; **186**: 1175–81.

95 Szurmant H, White RA, Hoch JA. Sensor complexes regulating two-component signal transduction. *Curr Opin Struct Biol* 2007; **17**: 706–15.

96 Schneider T, Gries K, Josten M *et al*. The lipopeptide antibiotic friulimicin B inhibits cell wall biosynthesis through complex formation with bactoprenol phosphate. *Antimicrob Agents Chemother* 2009; **53**: 1610–8.

97 Weiss EC, Zielinska A, Beenken KE *et al*. Impact of *sarA* on daptomycin susceptibility of *Staphylococcus aureus* biofilms *in vivo*. *Antimicrob Agents Chemother* 2009; **53**: 4096–102.

98 Ballal A, Ray B, Manna AC. sarZ, a sarA family gene, is transcriptionally activated by MgrA and is involved in the regulation of genes encoding exoproteins in *Staphylococcus aureus*. *J Bacteriol* 2009; **191**: 1656–65.